Near-Field thermal transistor InSb/WSM/InSb

D. Villamil-Malagón [1,*] and **E. Moncada-Villa** [1]

[1] *Escuela de Física, Universidad Pedagógica y Tecnológica de Colombia, Avenida Central del Norte 39-115, Tunja, Colombia*

*`deivid.villamil@uptc.edu.co`

ABSTRACT

Near-field radiative heat transfer has attracted increasing attention in recent years in the development and manufacturing of thermal devices analogous to the building blocks of current microelectronics. In this work, we study theoretically a near-field thermal transistor operating at room temperature. The source and drain were assumed as indium antimonide (InSb) plates, whereas the gate as a Weyl semimetal (WSM). Numerical results computed using the fluctuational electrodynamics framework indicate that the modulation and/or amplification of the heat flux in the considered transistor can be achieved by modifying the gate temperature, and by the action of an external magnetic field upon the system. Results obtained in this work make the proposed near-field thermal transistor a suitable candidate for the contactless devices for the heat flux control and thermal management at nanoscale.

Keywords: Near-Field Thermal Transistor, Thermotronics, Near-Field Radiative Heat Transfer, Thermal Management, Surface Waves, Magneto-Optic Medium, Weyl Semimetal.

1 INTRODUCTION

Two-body at different temperatures, and separated by a vacuum gap, can exchange heat via propagating and/or evanescent photons. The first exchange mechanism, known as far-field regime, is dominant as long as the separation between the bodies be much greater than the thermal wavelength, that is, the wavelength for which the energy density is maximum. However, at sub-wavelength distances (i.e., in the near-field regime) and in the presence of resonant surface modes, the main contributors to the transfer is given by the tunneling of evanescent photons. Such near-field radiative heat transfer (NFRHT) can exceed by several orders of magnitude the contribution of the propagating photons predicted by the Plank's blackbody radiation theory [1, 2]. This estimate of the NFRHT can be performed within framework of fluctuational electrodynamics [3, 4], which assumes that thermal radiation is generated by random electric currents inside the emitter body.

Experimental confirmation of the NFRHT [5, 6, 7], has triggered off the study and realization of thermal analogues to the building blocks of current microelectronics [8, 9], such as thermal diodes [10, 11] and thermal transistors [10, 12]. In this way, devices based on NFRHT has become of significant importance due to their ability to greatly increase the speed of information processing, since its transport is carried out through photons. In this regard, there have been several proposals for near-field thermal transistor (NFTT), consisting of three parallel plates separated by vacuum gaps, acting as the source, gate and drain of

the transistor, respectively. It has been demonstrated that in these systems, the modulation and/or amplification of the heat flux can be achieved as a result of the resonant tunneling through the gate of the evanescent field associated to surface modes in drain and collector [12, 10, 13]. Although there is experimental evidence of this behavior in the far-field regime [14], the experimental realization of the NFTT has not been completed yet.

As stated above, the NFRHT is linked to the resonant surface modes which in turn depends of the optical properties of the materials involved in the radiative thermal exchange. In this regard, a second approach for the control of NFRHT focuses on the research for the active control of the NFRHT via the dependence of the optical parameters with the temperature and/or external bias. A remarkable example of this concept is found in devices based on indium antimonide (InSb), whose dielectric function can be modified by the application of an external magnetic field, making this material a suitable candidate for the realization of a thermal diode [15]. Another example are the Weyl semimetals, which can support surface plasmon polaritons (SPP-WSM), and whose optical properties depend on temperature [16]. This material has been considered for the control of the NFRHT in a three-body system [17].

The goal of this work is the theoretical study of the of NFRHT in the near-field thermal transistor, InSb/WSM/InSb, illustrated in Fig. 1. We study the several operational modes of this device as a consequence of the variation of the different system parameters, such as the gate temperature, T_G, associated with the intermediate

film (body 2), and the application of an external magnetic field, H, which affects the optical properties of the InSb films playing the role of the source (body 1) and the drain (body 3). Furthermore, we also analyze the influence of geometrical parameters as the slab thicknesses, δ_j, and the size of the vacuum gap, d.
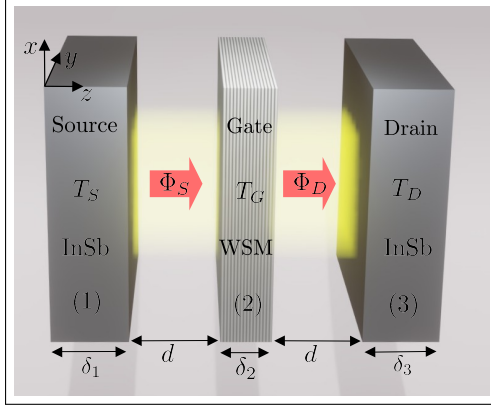

Fig. 1. Schematic representation of the proposed NFTT, consisting of three parallel films separated by a vacuum gap d. The source and drain are made of InSb, each with fixed temperatures T_S and T_D, respectively. Whereas the gate assumed to be a WSM and can operate at an adjustable temperature T_G. This system can be subjected to an external magnetic field along the z-axis.

The remaining of this paper is organized as follows. In the section 2, we present the specific details of the considered system and the theoretical framework used for the calculation of the radiative heat transport. In section 3, we discuss the main results, paying special attention to the operating modes of our proposed NFTT and the underlying mechanism for the amplification of the NFRHT. Main results are summarized in section 4.

2   RADIATIVE HEAT TRANSPORT IN A THREE PLATES SYSTEM: InSb/WSM/InSb

As explained in the Introduction, we focus on the study of a NFTT comprised by a magneto-optical material as InSb, and a topological semimetal. The optical properties of the InSb plates are described by the uniaxial dielectric tensor, $\varepsilon_{\text{InSb}} = \text{diag}(\varepsilon_1, \varepsilon_1, \varepsilon_2)$, where [18]

$$\varepsilon_1(H) = \varepsilon_\infty \left(1 + \frac{\omega_L^2 - \omega_T^2}{\omega_T^2 - \omega^2 - i\Gamma\omega} + \frac{\omega_p^2(\omega + i\gamma)}{\omega[\omega_c^2 - (\omega + i\gamma)^2]} \right),$$

$$\varepsilon_2 = \varepsilon_\infty \left(1 + \frac{\omega_L^2 - \omega_T^2}{\omega_T^2 - \omega^2 - i\Gamma\omega} - \frac{\omega_p^2}{\omega(\omega + i\gamma)} \right). \tag{1}$$

In this model the longitudinal and transverse optical phonons contributions are described by the frequencies ω_L and ω_T, respectively, and the free carriers by the plasma frequency ω_p. The influence of the magnetic field is given by the cyclotron frequency $\omega_c = eH/m^*$, where e denotes the electron charge and m^* its effective mass. All calculations in this work were

performed with the same parameters of Ref. [19], that is, $\varepsilon_\infty = 15.7$, $\omega_L = 3.62 \times 10^{13}$ rad/s, $\omega_T = 3.39 \times 10^{13}$ rad/s, $\Gamma = 5.65 \times 10^{11}$ rad/s, $\gamma = 3.39 \times 10^{12}$ rad/s, $n = 1.07 \times 10^{17}$ cm^{-3}, $\omega_p = 1.14 \times 10^{13}$ rad/s, and $m^*/m = 0.022$.

For the WSM slab, which is considered isotropic, its temperature-dependent dielectric function was assumed as $\varepsilon_{WSM} = \varepsilon_b + i\sigma/\Omega$, with [16, 20]

$$\sigma = \frac{r_s g}{6}\Omega G(\Omega/2) + i\frac{r_s g\Omega}{6\pi}\left\{ \frac{4}{\Omega^2}\left[1 + \frac{\pi^2}{3}\left(\frac{k_B T}{E_F}\right)^2 \right] \right.$$
$$\left. + 8\int_0^{\xi_c}\frac{G(\xi) - G(\Omega/2)}{\Omega^2 - 4\xi^2}\xi d\xi \right\}. \tag{2}$$

Here $G(E) = \frac{\sinh(E/Tk_B)}{\cosh(E_F/Tk_B) + \cosh(E/Tk_B)}$, E_F is the Fermi level, $\Omega = \hbar\omega/EF$, g is the number of Weyl nodes, $r_s = e^2/4\pi\varepsilon_0\hbar v_F$ is the effective fine structure constant, v_F is the Fermi velocity, and $\xi_c = E_c/E_F$, where E_c is the cutoff energy. In this work we used $E_F = 0.15$ eV, $v_F = 10^6$ m/s, $g = 4$, $\xi_c = 3$, $\varepsilon_b = 12$, as in Ref. [16].

Computation of the heat exchanges between the different plates in the proposed three-body system of Fig. 1, was carried out with the use of three-body model outlined in Ref. [13], according to which, the heat flux received by the drain, Φ_D, and the heat flux lost by the source, Φ_S, are given by

$$\Phi_D = \int_0^\infty \frac{d\omega}{2\pi}\sum_{\xi=\{s,p\}}\int_{ck>\omega}^\infty \frac{dk}{2\pi}k\left[\Theta_{12}\tau_\xi^{12} + \Theta_{23}\tau_\xi^{23}\right], \tag{3}$$

$$\Phi_S = \int_0^\infty \frac{d\omega}{2\pi}\sum_{\xi=\{s,p\}}\int_{ck>\omega}^\infty \frac{dk}{2\pi}k\left[\Theta_{32}\tau_\xi^{32} + \Theta_{21}\tau_\xi^{21}\right], \tag{4}$$

where $\Theta_{ij} = \Theta_i - \Theta_j$, $\Theta_i = \hbar\omega/[\exp(\hbar\omega/k_B T_i) - 1]$ is the occupation of the photon states in the i−th slab at a temperature T_i, and k is the magnitude of the wave vector parallel to the surface of the slabs. Functions $\tau_\xi^{ij}(\omega, k, d)$ denotes the transmission probability of evanescent photons from i-th to the j-th plate. These probabilities can be written in terms of optical reflection coefficients, ρ_ξ^j, and transmission coefficients, τ_ξ^j, of each individual element of the system [13], as well as the reflection coefficients for the coupled elements, ρ_ξ^{12}, in the following form

$$\tau_\xi^{12} = \frac{4|\tau_\xi^2|^2 \text{Im}(\rho_\xi^1)\text{Im}(\rho_\xi^3)e^{-4\text{Im}(q_0)d}}{|1 - \rho_\xi^{12}\rho_\xi^3 e^{-2\text{Im}(q_0)d}|^2 |1 - \rho_\xi^1\rho_\xi^2 e^{-2\text{Im}(q_0)d}|^2}, \tag{5}$$

$$\tau_\xi^{23} = \frac{4\text{Im}(\rho_\xi^{12})\text{Im}(\rho_\xi^3)e^{-2\text{Im}(q_0)d}}{|1 - \rho_\xi^{12}\rho_\xi^3 e^{-2\text{Im}(q_0)d}|^2}. \tag{6}$$

In the preceding expressions, ξ denotes the polarization state (s or p), $q_0 = \sqrt{\omega^2/c^2 - k^2}$ is the wave vector component perpendicular to the plates surfaces and c is the velocity of light in the vacuum. It is important to mention that transmission probabilities τ_ξ^{21} and τ_ξ^{32} are obtained by exchanging indexes $2 \leftrightarrow 1$ and $3 \leftrightarrow 2$ in equations (5) and (6), respectively.

Heat fluxes given by Eqs. (3) and (4) allow us to compute the net heat flux received or emitted by gate as [12, 21]

$$\Phi_G = |\Phi_S| - |\Phi_D|. \tag{7}$$

Notice that this three-body model described above can also be applied for the calculation of the heat flux in a two-body system (InSb/InSb) separated by a gap, by simply making $d_{2b} = 2d$ and $\delta_2 = 0$. In this case, $\Phi_2(d_{2b}) \equiv \Phi_D(d, \delta_2 = 0) = \Phi_S(d, \delta_2 = 0)$. Using this limit, the amplification of the NFTT can be expressed in terms of the ratio [13]

$$\frac{\Phi_D(d, \delta_2)}{\Phi_2(2d + \delta_2)} > 1. \tag{8}$$

3 RESULTS AND DISCUSSION

With the use of the theoretical model outlined in the preceding section, we have calculated the heat fluxes, Eqs. (3)-(7), for *p*-polarized waves, assuming a symmetric configuration, that is, $\delta_1 = \delta_3 = 80$ nm and $d = 50$ nm. The temperatures of the source and drain were assumed as $T_1 = 320$ K and $T_3 = 300$ K, respectively, for all the calculations, whereas the gate temperature, T_2, is modulated between these two values, that is, $T_1 > T_2 > T_3$.

In Figs. 2 and 3 the main results are presented as a function of gate temperature and applied magnetic field, respectively. We show in panels (a), (b) and (c) the heat flux received or lost by the source, gate and drain, respectively. These results are used for the calculation of the amplification factor (see panel (d)) relative to the two-body system.
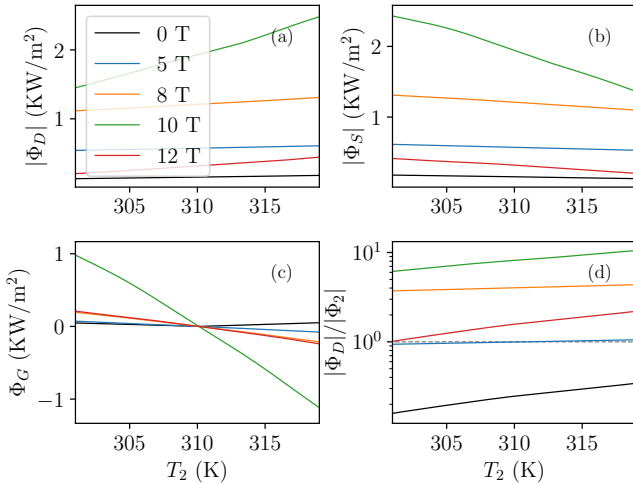
Fig. 2. Radiative heat flux as a function of gate temperature for various applied magnetic field values and a gate thickness of $\delta_2 = 80$ nm. (a) Heat flux received by the drain, (b) heat flux lost by the source, (c) heat flux exchanged by the gate, and (d) radiative heat transfer amplification.
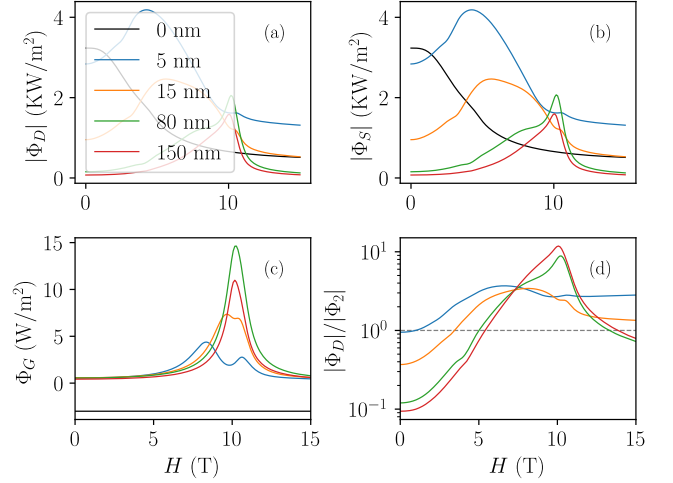
Fig. 3. Radiative heat flux as a function of the external magnetic field for various gate thickness values with a fixed temperature of $T_2 = 310$ K. (a) Heat flux received by the drain, (b) heat flux lost by the source, (c) heat flux exchange at the gate, and (d) radiative heat transfer amplification.

3.1 Operating Modes

Modulation: Obtained results suggest that the modulation of radiative heat flux in the proposed NFTT can be achieved by manipulating the gate temperature and/or by the action of an external magnetic field. This is evident in panels (a), (b) y (c) of Figs. 2 and 3, where the fluxes in all configurations change when either of these two parameters varies. It can be observed that the temperature-induced modulation is more pronounced for a magnetic field value of $H = 10$ T (green line in Fig. 2).

Amplification: The most remarkable characteristic of a transistor is its ability to amplify the heat flux from the source to the drain. In panel (d) of Figs. 2 and 3, the calculation of the amplification of the proposed NFTT is presented for different system parameters. It can be observed that the proposed NFTT amplifies ($\Phi_D/\Phi_2 > 1$) primarily for a magnetic field intensity of $H = 10$ T. By selecting the appropriate parameters, the amplification can reach values close to 15 compared to the two-body system.

3.2 Underlying Mechanisms

For a deeper insight of the role of the gate in the enhancement of the NFRHT, we plotted in Fig. 4 the transmission probabilities for different gate thicknesses (in columns) and different magnetic field values (in rows), $\tau_3 \equiv (\tau_p^{12} + \tau_p^{23})/2$. In the absence of a magnetic field (first row), the coupling between the InSb surface modes (PSs-InSb) and the SPP-WSM is not optimal. Furthermore, the PSs-InSb modes shown in panel (a), which reside in the lower frequency range, are attenuated by the presence of the gate, especially as its thickness increases. As can be seen from panels (b) and (c), despite an additional mode (SPP-WSM) emerging around $\omega = 7 \times 10^{13}$ rad/s when the gate is situated, the peaks of PSs-InSb decrease to smaller

values of k. In this configuration, the gate can act as a resistive barrier [22] that obstructs the transmission of InSb surface modes from the source to the drain as its thickness increases by a few nanometers. In contrast, when a 5 T magnetic field is applied, the coupling between hyperbolic modes [see Fig. 4(d)] induced in the InSb plates (HM-InSb) and the lower region of the SPP-WSM, occurring around $\omega = 4.9 \times 10^{13}$ rad/s, is enhanced, as shown in Figs. 4(e) and 4(f). This improvement becomes even more significant with a 10 T field. At 10 T, the HM-InSb modes shift towards higher frequencies [see Fig. 4(g)], close to the frequency of the SPP-WSM, approximately at $\omega = 8.2 \times 10^{13}$ rad/s, as seen in Figs. 4(h) and 4(i). In these Figs., the SPP-WSM is largely overlapped by the HM-InSb. Moreover, it's noticeable that as the gate thickness increases [see Fig. 4(i)], the coupling between the SPP-WSM and MH-InSb becomes more pronounced in that region, suggesting that the enhancement of NFRHT is attributed to the tunneling of evanescent photons by the gate.
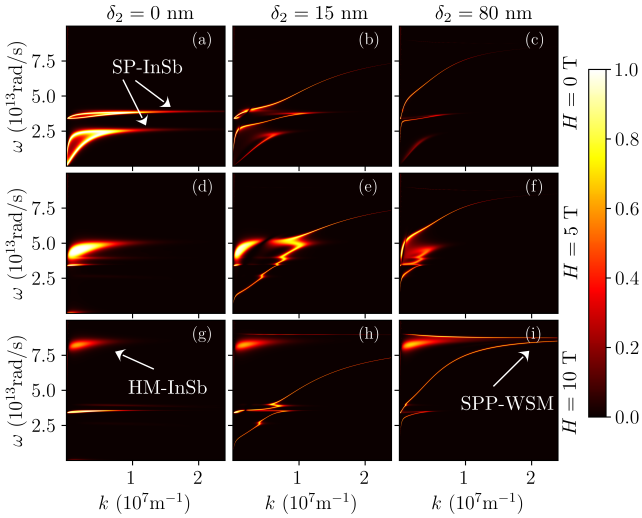

Fig. 4. Transmission probability τ_p^{13} for different magnetic field values (in rows) and various gate thicknesses (in columns). Different resonant modes are also indicated.

4   CONCLUSIONS

We focused on study of the behavior of NFRHT in the three-body system: InSb/WSM/InSb, which exhibits characteristics of a NFTT due to the presence of a magneto-optical material and a Weyl semimetal. The calculations have demonstrated that the modulation of radiative heat flux can be achieved by manipulating the gate temperature and applying a magnetic field. Furthermore, amplification between the source and drain can be attained in comparison to its two-body counterpart, facilitated by the tunneling of evanescent photons from the gate. This work contributes to the developing of non-contact functional thermal devices, including thermal logic gates and memory devices.

Declaration: The authors have no conflicts to disclose.

REFERENCES

[1] J. C. Cuevas and F. J. García-Vidal, "Radiative heat transfer," *ACS Photonics*, vol. 5, no. 10, pp. 3896–3915, 2018.

[2] S.-A. Biehs, R. Messina, P. S. Venkataram, A. W. Rodriguez, J. C. Cuevas, and P. Ben-Abdallah, "Near-field radiative heat transfer in many-body systems," *Rev. Mod. Phys.*, vol. 93, p. 025009, 2021.

[3] D. Polder and M. Van Hove, "Theory of radiative heat transfer between closely spaced bodies," *Phys. Rev. B*, vol. 4, pp. 3303–3314, 1971.

[4] M. Francoeur and M. Pinar Mengüç, "Role of fluctuational electrodynamics in near-field radiative heat transfer," *J. Quant. Spectrosc. Radiat. Transf.*, vol. 109, no. 2, pp. 280–293, 2008.

[5] A. Narayanaswamy, S. Shen, and G. Chen, "Near-field radiative heat transfer between a sphere and a substrate," *Phys. Rev. B*, vol. 78, p. 115303, 2008.

[6] M. Lim, S. S. Lee, and B. J. Lee, "Near-field thermal radiation between doped silicon plates at nanoscale gaps," *Phys. Rev. B*, vol. 91, p. 195136, 2015.

[7] B. Song, Y. Ganjeh, S. Sadat, D. Thompson, A. Fiorino, V. Fernández-Hurtado, J. Feist, F. J. Garcia-Vidal, J. C. Cuevas, P. Reddy, and E. Meyhofer, "Enhancement of near-field radiative heat transfer using polar dielectric thin films," *Nat. Nanotechnol.*, vol. 10, no. 3, pp. 253–258, 2015.

[8] P. Ben-Abdallah and S.-A. Biehs, "Thermotronics: Towards nanocircuits to manage radiative heat flux," *Zeitschrift für Naturforschung A*, vol. 72, no. 2, pp. 151–162, 2017.

[9] G. Wehmeyer, T. Yabuki, C. Monachon, J. Wu, and C. Dames, "Thermal diodes, regulators, and switches: Physical mechanisms and potential applications," *Appl. Phys. Rev.*, vol. 4, no. 4, p. 041304, 2017.

[10] E. Moncada-Villa and J. C. Cuevas, "Normal-metal–superconductor near-field thermal diodes and transistors," *Phys. Rev. Appl.*, vol. 15, p. 024036, 2021.

[11] P. Ben-Abdallah and S.-A. Biehs, "Phase-change radiative thermal diode," *Appl. Phys. Lett.*, vol. 103, no. 19, p. 191907, 2013.

[12] P. Ben-Abdallah and S.-A. Biehs, "Near-field thermal transistor," *Phys. Rev. Lett.*, vol. 112, p. 044301, 2014.

[13] R. Messina, M. Antezza, and P. Ben-Abdallah, "Three-body amplification of photon heat tunneling," *Phys. Rev. Lett.*, vol. 109, p. 244302, 2012.

[14] Y. Li, Y. Dang, S. Zhang, X. Li, Y. Jin, P. Ben-Abdallah, J. Xu, and Y. Ma, "Radiative thermal transistor," *Phys. Rev. Appl.*, vol. 20, p. 024061, 2023.

[15] D. Feng, S. K. Yee, and Z. M. Zhang, "Near-field photonic thermal diode based on hBN and InSb films," *Appl. Phys. Lett.*, vol. 119, no. 18, p. 181111, 2021.

[16] O. V. Kotov and Y. E. Lozovik, "Dielectric response and novel electromagnetic modes in three-dimensional dirac semimetal films," *Phys. Rev. B*, vol. 93, p. 235417, 2016.

[17] Z. Yu, X. Li, T. Lee, and H. Iizuka, "Near-field radiative heat transfer in three-body weyl semimetals," *Opt. Express*, vol. 30, no. 18, pp. 31584–31601, 2022.

[18] E. D. Palik, R. Kaplan, R. W. Gammon, H. Kaplan, R. F. Wallis, and J. J. Quinn, "Coupled surface magnetoplasmon-optic-phonon polariton modes on insb," *Phys. Rev. B*, vol. 13, pp. 2497–2506, 1976.

[19] E. Moncada-Villa, V. Fernández-Hurtado, F. J. García-Vidal, A. García-Martín, and J. C. Cuevas, "Magnetic field control of near-field radiative heat transfer and the realization of highly tunable hyperbolic thermal emitters," *Phys. Rev. B*, vol. 92, p. 125418, 2015.

[20] O. V. Kotov and Y. E. Lozovik, "Giant tunable nonreciprocity of light in weyl semimetals," *Phys. Rev. B*, vol. 98, p. 195446, 2018.

[21] Y. H. Kan, C. Y. Zhao, and Z. M. Zhang, "Near-field radiative heat transfer in three-body systems with periodic structures," *Phys. Rev. B*, vol. 99, p. 035433, 2019.

[22] N. Zolghadr and M. Nikbakht, "Radiative resistance at the nanoscale: Thermal barrier," *Phys. Rev. B*, vol. 102, p. 035433, 2020.